Detection of gray matter microstructural changes in Alzheimer's disease continuum using fiber orientation

Peter Lee
Korea Advanced Institute of Science and Technology https://orcid.org/0000-0001-5433-1882
Hang-Rai Kim
Korea Advanced Institute of Science and Technology
Yong Jeong (yong@kaist.ac.kr)
https://orcid.org/0000-0002-5907-3787

Research article

Keywords: Alzheimer's disease, Early diagnosis, Diffusion tensor imaging, Microstructure, Biomarkers

Posted Date: June 15th, 2020

DOI: https://doi.org/10.21203/rs.3.rs-17303/v4

Version of Record: A version of this preprint was published on October 2nd, 2020. See the published version at https://doi.org/10.1186/s12883-020-01939-2.

Abstract

Background: This study aims to investigate feasible gray matter microstructural biomarker with higher sensitivity for early Alzheimer's disease (AD) detection. We propose diffusion tensor imaging (DTI) measure, 'radiality', for early AD biomarker. It is a dot product between cortical surface normal vector and primary diffusion direction, which reflects the fiber orientation within the cortical column.

Methods: We gathered neuroimages from the Alzheimer's Disease Neuroimaging Initiative (ADNI) database: 78 cognitive normal, 50 early mild cognitive impairment (EMCI), 34 late mild cognitive impairment (LMCI), and 39 AD patients. Then, we evaluated cortical thickness (CTh), mean diffusivity (MD), amount of amyloid and tau accumulations using positron emission tomography (PET), which are conventional AD magnetic resonance (MR) imaging biomarkers. Radiality was projected on gray matter surface to compare and validate the changes along stages with other neuroimage biomarkers.

Results: Results showed decreased radiality primarily in entorhinal, insula, frontal and temporal cortex as disease progresses onward. Especially, radiality could delineate the difference between cognitive normal and EMCI group while other biomarkers could not. We looked into the relationship between the radiality and other biomarkers to validate its pathological evidence in AD. Overall, radiality showed high association with conventional biomarkers. Additional ROI analysis exhibits dynamics of AD related changes as stages onward.

Conclusion: Radiality in cortical gray matter showed AD specific changes and relevance with other conventional AD biomarkers with higher sensitivity. Besides, it could show group differences in early AD changes from EMCI which show advantage for early diagnosis than using conventional biomarkers. We provide the evidence of structure changes with cognitive impairment and suggest radiality as a sensitive biomarker for early AD.

1. Background

Alzheimer's disease (AD) is notorious for its long preclinical period where various pathophysiological changes occur before the main symptom. As progress of AD is not completely understood, early diagnosis and intervention remain hopeless [1, 2]. Repetitive failures of recent drug trials attribute to applying treatment to patients at the progressed stage [3-5]. Thus, identification of people at the earlier stage is critical in clinical trials and may be promising for controlling this devastating disease.

At present, there are several biomarkers to diagnose and monitor disease progression: amyloid and tau deposit through positron emission tomography (PET) imaging or from cerebrospinal fluid (CSF), volumetric and morphology analysis using T1 weighted magnetic resonance (MR) imaging and clinical assessments. Although the results from PET and CSF screening are promising, these interventions are more invasive than MR imaging. In the urge of finding suitable MR biomarkers, researchers have focused on characterizing early mild cognitive impairment (EMCI) and late mild cognitive impairment (LMCI) [6-7]. Although the criteria to separate EMCI and LMCI was based on the memory score, biomarkers from EMCI

showed continuous spectrum to LMCI implying that EMCI as a transitional stage of AD [8]. Thus, evaluating the sequential changes of EMCI and LMCI should help understanding the early AD.

Diffusion tensor imaging (DTI) utilizes the diffusion of water molecules within tissues and provides axonal microstructural properties, thus widely applied for studying white matter integrity [9, 10]. Early AD studies using DTI have studied mainly on the white matter. However, since white-matter changes in AD may be the results of Wallerian degeneration, followed by the neurodegeneration in gray matter [11, 12], the destruction of white matter is a less sensitive change in AD.

The idea of measuring microstructural changes in gray matter using DTI has been demonstrated in both AD and frontotemporal dementia [13-15]. These studies showed that gray matter mean diffusivity (MD) is increased in patients compared with healthy control and MD could be a promising imaging biomarker. However, there is lasting notion that increased MD could be overestimated by CSF signal and this effect persisted even with rigorous correction such as partial volume effects correction [16].

To overcome this problem, we adopted radiality, which is presumably reflecting the integrity of tangential cortical fibers. As an initial study to apply radiality in AD, we sought to find association with conventional MR biomarkers [17]. Recent study investigated the association between anisotropic diffusion and cortical structure through postmortem diffusion MR imaging along with histology in multiple sclerosis [18]. Although this study limited to observe certain brain regions, it provides relevant evidences to measure cortical changes with DTI. Moreover, this parameter has been applied to study neurodevelopment and could distinguish stages of aging [19-21]. Cortical microstructural changes are often observed with aging or neurodegeneration, which can be viewed as opposite of neurodevelopment [22, 24-26]. Thus, changes of fiber orientation may suggest cortical alterations and could be used as a biomarker in the neurodegenerative diseases.

In this study, we hypothesized that the radiality within gray matter could be a microstructural measure of cortex and used as the early signature of AD. We performed a cross-sectional surface-based cortical analysis approach using DTI, amyloid PET, and Tau PET images to AD continuum [17]. We evaluated whether gray matter radiality shows: i) early mesoscopic AD-related pathological change, and ii) compliment to conventional AD biomarkers while providing a distinct information regarding AD-related pathologies.

2. Methods

2.1 Demographics

Data used in this study were obtained from Alzheimer's Disease Neuroimaging Initiative (ADNI) (adni.loni.usc.edu). Among ADNI database, we analyzed the subjects who took both MRI and PET (amyloid, AV 45 and tau, AV 1451): 78 cognitive normal (CN), 50 EMCI, 34 LMCI, and 39 AD. Subjects were sampled with following criteria: age around 60 to 90-year-old, education year 12 to 20, and gender match within group. To assess AD continuum, amyloid negative CN and amyloid positive EMCI, LMCI, and AD

subjects were selected. EMCI group was subdivided into 38 dementia non-converter (stable EMCI) and 12 converter group to assess changes with disease progression. A total of 201 subjects' T1 and DTI images were gathered from ADNI. To increase sample size, multi-center approach was used as discussed in [13]. The amyloid positivity of the subjects was determined by whole brain PET AV45 standardized uptake value ratio (SUVR) with 1.11 cut-off. **Table 1** shows the demographics of the subjects used in this study; note that subjects who underwent AV1451 tau PET imaging were 44 in CN, 9 in EMCI, 5 in LMCI, and 3 in AD. Additional 28 CN subjects who showed amyloid positive were gathered to identify earliest AD pathological changes as presented in **Supp. Table 1**.

2.2 Image processing

T1 weighted images were processed with Freesurfer package v6.0 (http://surfer.nmr.mgh.harvard.edu) as previously reported in [13]. Cortical thickness (CTh) maps were registered to Freesurfer average sphere through spherical registration for group comparison. DTI and PET images were registered with their respect to T1 images using boundary-based algorithm for further process. DTI images were processed using FSL package as followed: eddy current correction, rotate gradient vectors from the results of eddy correction, and tensor fitting to produce mean diffusivity map and primary eigenvector map. DTI metrics were further processed to avoid partial volume effect using Koo et al [27]. PET images were partial volume corrected using mri_gtmpvc which is built in Freesurfer package. PET images were normalized by mean signal from whole cerebellum and converted to SUVR for amyloid and tau PET, AV45 and AV1451 respectively. Then images were boundary-based registered to corresponding T1 structural images. To avoid any partial volume effects, the center parts of the cortical column were sampled for surface analysis. Lastly, CTh was smoothed with 10 mm while other modalities were smoothed with 15 mm full width half maximum Gaussian kernel. **Fig. 1** shows the overall scheme of the process.

2.3 Calculation of radiality

A surface normal vector was obtained from individual gray matter surface to define cortical orientation. Freesurfer represent the surface in triangular meshes, and surface normal vector can be computed using cross-product between edges. Vertex-wise dot product between primary diffusion direction, primary eigenvector of diffusion tensor, and the surface normal vector was quantified as a radiality index: r. where v represents surface normal vector and e1 represents primary diffusion direction [22].

See formula 1 in the supplementary files.

It ranges from 0 to 1, where r = 0 indicates tangential diffusion and r = 1 indicates radial diffusion to cortex. Subject's principal eigenvector map was projected onto the individual surface reconstruction to calculate vertex-wise radiality as discussed in [22].

2.4 Cut-off analysis

To further test feasibility of radiality as AD biomarker, we performed cut-off analysis using receiver operating characteristics graphs to distinguish CN with other AD stages as shown in **Supp. Table 2.** The

feature used was the mean radiality within cluster that obtained from CN vs EMCI group comparison. With varying cut-off, we sought to find the cost-effective point where it minimizes the difference between sensitivity and specificity [23].

2.5 Statistical analysis

We first compared the differences between groups for radiality, CTh, MD, AV45 and AV1451 with a general linear model, which is available in Freesurfer. The results were cluster-wise corrected for family-wise error (FWE) corrected *p*-value < 0.05

To test the associations between radiality and other neuroimage biomarkers, we calculated set of vertex-wise partial correlations with the radiality as the dependent variable and CTh, MD, AV45, and AV1451 as the independent variable. Age, gender, year of education, and MRI center were set as covariates of cluster analyses. Permutation test was applied to resolve multiple comparisons problem through a Monte Carlo simulation with 10,000 repeats, which is built-in function of Freesurfer.

To test the linear relationship between radiality and other neuroimage biomarkers, we quantified mean metrics within AD specific ROIs. ROIs include entorhinal, fusiform, insula, inferior, middle, and superior temporal cortex. Mean metrics within ROIs were plotted in a box and whisker plots and presented in **Fig. 5(e)** and **Fig. 6**. Significance between groups was tested with one-way ANOVA.

3. Results

3.1 Group comparison along AD continuum

We first compared radiality, CTh, and MD differences between groups: CN vs EMCI, CN vs LMCI, and CN vs AD as respectively. The results were cluster-wise corrected for FWE corrected *p*-value < 0.05. **Fig. 2** shows significant group different clusters range from *p*-value 0.05 to 10^{-5}. Only radiality could delineate the difference from EMCI to CN. Compared to CN, all groups showed decreased radiality, decreased CTh, and increased MD. There was no group difference of radiality between EMCI and LMCI.

3.2 EMCI non-converter versus converter

We compared radiality between groups: CN vs EMCI non-converter, CN vs EMCI converter, and EMCI non-converter vs converter as respectively. The results were cluster-wise corrected for FWE corrected *p*-value < 0.05. **Fig. 3** shows significant group different clusters range from *p*-value 0.05 to 10^{-5}. Compared to CN, EMCI non-converter showed decreased radiality in left superior frontal and superior parietal cortex. EMCI converter showed decreased radiality mainly in bilateral insula cortex. Direct comparison between EMCI non-converter and converter delineated bilateral insular, left superior frontal, and right precentral cortex.

3.3 Partial correlation between radiality and other image biomarkers

We then found vertex-wise correlation between radiality and other image biomarkers as shown in **Fig. 4**. CTh showed mostly positive correlations that decrease in cortical thickness accompanied with decrease in radiality. MD showed mostly negative correlation that increase in MD accompanied with decrease in radiality. Amyloid and tau levels showed negative correlation with radiality.

3.4 Correlations between radiality and other image biomarkers

In order to find progressive changes in radiality as disease progression, AD specific ROIs mask was used to calculate mean biomarker data. Each subject's mean data were scatter plotted and used to calculate Pearson correlation as shown in **Fig. 5**. CTh showed R = 0.641, MD showed R = -0.677, AV45 showed R = -0.490, and AV1451 showed R = -0.412 with radiality.

3.5 Radiality dynamics from AD specific ROIs

To find generative changes in radiality as disease progresses, mean radiality in AD ROIs was calculated for direct comparison among groups. Radiality within AD specific ROIs were plotted in a box and whisker plot as shown in **Fig. 6**. The results showed decreasing radiality with disease progression. Significance was tested with one-way ANOVA with p-value < 0.05, 0.01, 0.001. Insula, middle and superior temporal cortex showed most radiality reduction with disease onward.

3.6 Cut-off analysis using Radiality

Classification of CN vs EMCI showed 70.5% accuracy with 70.2% sensitivity, 72.7% specificity, and 0.766 AUC. Subsequent analysis to distinguish between CN and LMCI, MCI group (EMCI+LMCI), AD, and patient group (EMCI+LMCI+AD) also showed similar results presented in **Supp. Table 2.**

4. Discussion

In this study, we tried to investigate the early features of EMCI using cortical radiality, which reflects mesoscopic structural changes. By leveraging the radiality in the gray matter, we could detect the changes in EMCI which were not detected by conventional MRI biomarkers. We found progressively larger regions of decreased radiality as disease progresses, starting from medial temporal cortex in EMCI to whole brain in AD. While, CTh or MD did not show significant differences between CN and EMCI. Furthermore, the radiality result from CN and EMCI non-converter showed similar pattern with those of CN amyloid negative and positive (**Supp. Fig. 1**). Based on our results, the microstructural gray matter changes in bilateral insula cortex are associated with the disease progression as presented in CN and EMCI-converter result.

We investigated the relationship of radiality with other image measures. Association between radiality and CTh showed strong positive correlation on widespread regions of the brain as shown in **Fig. 4**. It is clear that higher CTh indicate deeper cortical structure and fiber orientation tend to have radial orientation. Cortical depth profile analysis showed that thicker the cortical thickness larger the radiality [28]. In addition, MD showed strong negative correlation on mostly temporal, parietal, and frontal cortices.

Radiality may sensitive to CTh but reflecting microstructural feature as well. With AV45 and AV1451, radiality showed association that widely overlapped with both CTh and MD. Thus, radiality may also reflect changes due to accumulation of pathologic protein accumulation within the cortex.

Although microstructural changes associated with radiality is unclear, one plausible feature is the disorganization of tangential cortical fibers. It has been reported that the tangential cortical fibers develop at the stages of neurodevelopment and aging [22]. There are several events that lead to increase in tangentially oriented fibers including dendritic elaboration [29], formation of local circuits [30], expansion of thalamo-cortical fibers [31] and disappearance of radial glia [32, 33]. Decrease in radiality may indicate contrary to those of neurodevelopment. For instance, synaptic loss, neuronal soma changes and neurite disorganization occurs along with the neuronal loss may lead to decrease in radiality. These changes may concurrent with net loss of macromolecule that affect diffusivity, increasing free water in extracellular space. However, radiality provides evidence of neuronal density that explains concurrent cortical atrophy. Furthermore, accumulation of amyloid or tau proteins may also participate in the disruption of microstructure. Given radiality can delineate the EMCI, we can further speculate that these microstructural changes occur in the earlier stage of AD which are not apparent in macroscopic investigation.

To test the sensitivity of radiality, we sought to find earliest stage of AD. Interestingly, our CN vs EMCI radaility analysis did not show biphasic trajectory as discussed in previous work [34]. Thus, we conducted additional analysis on amyloid negative CN and amyloid positive CN (**Supp Fig. 1**). We could observe biphasic behavior of CTh and MD where biomarkers showed opposite direction of changes. While CTh showed increased and MD decreased, radiality showed monotonous decrease in amyloid positive CN. This distinct behavior of radiality could characterize the changes in EMCI while CTh and MD could not. Both the CTh increase and MD decrease in early stage of AD was thought to be caused by an amyloid-induced inflammatory response [13]. However, radiality seems to decrease whenever there are microstructural changes in the tissue. From preterm study, occipital cortex showed decrease in radiality as in early development [19-21]. In the case of multiple sclerosis, decreased radiality was observed in dorsolateral prefrontal cortex, Heschl's gyrus, and primary visual cortex possibly due to cortical alterations [18].

We performed simple cut-off binary classification analysis to assess diagnostic accuracy of radiality. The target mask was obtained from the group comparison result of CN versus EMCI, and individual mean radiality within mask was used as a classification feature. With varying cut-off, the model showed 70.5% accuracy with 0.766 AUC to differentiate CN and EMCI, 67.9% with 0.757 AUC to CN and LMCI, 70.5% with 0.766 AUC to CN and MCI (EMCI+LMCI), and 78.6% with 0.867 AUC to CN and AD as presented in **Supp. Table 2**. The results were comparable to previous studies. Recent study adopted logistic regression model with neurite density index, orientation dispersion index, and CTh as features reported 0.72 AUC to CN and MCI and 0.91 AUC to CN and AD [35]. Other studies employing whole MD and gray matter map reported: 79.6% accuracy with 0.84 AUC to CN and MCI and 93.5% with 0.94 AUC to CN and AD [36], 76% with 0.83 AUC to NC and AD [37].

There were several limitations of the current study. First, relatively poor resolution of DTI images compared to structural T1 could lead inaccurate results. Although surface analysis was employed to mitigate registration or segregation error, higher resolution of DTI would be needed to observe precise cortical changes. Second, use of multi-protocol DTI images could influence the observation of progressive changes in MCI. We sought to control age, gender, year of education, and MRI center variate among the group while applying harmonization to minimize the variation between subjects [38]. Third, number of subjects who took tau PET imaging were not enough to show the relationship with tau pathology. In order to focus on progressive changes, not only showing relationship with amyloid but also with tau is important aspect [39]. However, several subjects in this study underwent screening only once without follow up or only MRI data were available.

5. Conclusions

In conclusion, we investigated the cortical changes in EMCI using structural MRI and DTI as well as PET imaging markers. Only radiality could delineate the changes in EMCI while cortical thickness and MD could not. In addition, radiality changes in frontal cortex as simultaneously with amyloid deposit in continuum. These results indicate that multimodal approach, atrophy and microstructure, may illuminate early changes in AD. However, further study is needed to support the relationship between cortical structure alterations and diffusion orientation changes.

Declarations

Ethical approval and consent to participate

The study procedures were approved by the institutional review boards of all participating centers (https://adni.loni.usc.edu/wp-content/uploads/how_to_apply/ ADNI_Acknowledgement_List.pdf), and written informed consent was obtained from all participants or their authorized representatives. Ethics approval was obtained from the institutional review boards of each institution involved: Oregon Health and Science University; University of Southern California; University of California—San Diego; University of Michigan; Mayo Clinic, Rochester; Baylor College of Medicine; Columbia University Medical Center; Washington University, St. Louis; University of Alabama at Birmingham; Mount Sinai School of Medicine; Rush University Medical Center; Wien Center; Johns Hopkins University; New York University; Duke University Medical Center; University of Pennsylvania; University of Kentucky; University of Pittsburgh; University of Rochester Medical Center; University of California, Irvine; University of Texas Southwestern Medical School; Emory University; University of Kansas, Medical Center; University of California, Los Angeles; Mayo Clinic, Jacksonville; Indiana University; Yale University School of Medicine; McGill University, Montreal-Jewish General Hospital; Sunnybrook Health Sciences, Ontario; U.B.C.Clinic for AD & Related Disorders; Cognitive Neurology—St. Joseph's, Ontario; Cleveland Clinic Lou Ruvo Center for Brain Health; Northwestern University; Premiere Research Inst (Palm Beach Neurology); Georgetown University Medical Center; Brigham and Women's Hospital; Stanford University; Banner Sun Health Research Institute; Boston University; Howard University; Case Western Reserve University; University of California,

Davis—Sacramento; Neurological Care of CNY; Parkwood Hospital; University of Wisconsin; University of California, Irvine—BIC; Banner Alzheimer's Institute; Dent Neurologic Institute; Ohio State University; Albany Medical College; Hartford Hospital, Olin Neuropsychiatry Research Center; Dartmouth-Hitchcock Medical Center; Wake Forest University Health Sciences; Rhode Island Hospital; Butler Hospital; UC San Francisco; Medical University South Carolina; St. Joseph's Health Care Nathan Kline Institute; University of Iowa College of Medicine; Cornell University; and University of South Florida: USF Health Byrd Alzheimer's Institute. Upon accessing the database, we have received administrative approval for access to the ADNI database.

Consent for publication

Not applicable

Availability of data and materials

The MRI and PET data were downloaded from the Alzheimer's Disease Neuroimaging Initiative (ADNI) database (http://adni.loni.usc.edu/). Application for access to the ADNI data can be submitted by anyone at http://adni.loni.usc.edu/data-samples/access-data/. The process includes completion of an online application form and acceptance of Data Use Agreement.

Competing interests

The authors declare that they have no competing interests.

Funding

Data analysis, result interpretation, and manuscript writing were supported in part by grant HI14C2768 from the Korea Health Technology Research and Development Project through the Korea Health Industry Development Institute, funded by the Ministry of Health & Welfare, Republic of Korea. Data analysis, method development, and manuscript writing were supported in part by the Bio & Medical Technology Development Program (2016941946) through the National Research Foundation of Korea (NRF), funded by the Ministry of Science, ICT and Future Planning.

Data collection and designing for this project was funded by the Alzheimer's Disease Neuroimaging Initiative (ADNI) (National Institutes of Health Grant U01 AG024904) and DOD ADNI (Department of Defense award number W81XWH-12-2-0012). ADNI is funded by the National Institute on Aging, the National Institute of Biomedical Imaging and Bioengineering, and through generous contributions from the following: AbbVie, Alzheimer's Association; Alzheimer's Drug Discovery Foundation; Araclon Biotech; BioClinica, Inc.; Biogen; Bristol-Myers Squibb Company; CereSpir, Inc.; Eisai Inc.; Elan Pharmaceuticals, Inc.; Eli Lilly and Company; EuroImmun; F. Hoffmann-La Roche Ltd and its affiliated company Genentech, Inc.; Fujirebio; GE Healthcare; IXICO Ltd.; Janssen Alzheimer Immunotherapy Research & Development, LLC.; Johnson & Johnson Pharmaceutical Research & Development LLC.; Lumosity; Lundbeck; Merck & Co., Inc.; Meso Scale Diagnostics, LLC.; NeuroRx Research; Neurotrack Technologies; Novartis

Pharmaceuticals Corporation; Pfizer Inc.; Piramal Imaging; Servier; Takeda Pharmaceutical Company; and Transition Therapeutics. The Canadian Institutes of Health Research is providing funds to support ADNI clinical sites in Canada. Private sector contributions are facilitated by the Foundation for the National Institutes of Health (www.fnih.org). The grantee organization is the Northern California Institute for Research and Education, and the study is coordinated by the Alzheimer's Disease Cooperative Study at the University of California, San Diego. ADNI data are disseminated by the Laboratory for Neuro Imaging at the University of Southern California.

Authors' contributions

PL, YJ, and HK contributed to the study conception and design. Material preparation, data collection and analysis were performed by PL. The first draft of the manuscript was written by PL. YJ and HK commented on previous versions of the manuscript. All authors read and approved the final manuscript.

Acknowledgement

Data used in preparation of this article were obtained from the Alzheimer's Disease Neuroimaging Initiative (ADNI) database (adni.loni.usc.edu). As such, the investigators within the ADNI contributed to the design and implementation of ADNI and/or provided data but did not participate in analysis or writing of this report. A complete listing of ADNI investigators can be found at: http://adni.loni.usc.edu/wp-content/uploads/how_to_apply/ADNI_Acknowledgement_List.pdf

Abbreviations

AD Alzheimer's disease

MD Mean diffusivity

ADNI Alzheimer's Disease Neuroimaging Initiative

EMCI Early mild cognitive impairment

LMCI Late mild cognitive impairment

CTh Cortical thickness

PET Positron emission tomography

CSF Cerebrospinal fluid

MR Magnetic resonance

DTI Diffusion tensor imaging

CN Cognitive normal

GCDR Global clinical dementia ratings

MMSE Mini Mental State Examination

MADAS-Cog Modified Alzheimer's disease Assessment Scale cognitive subscale

SUVR Standardized uptake value ratio

ROI Region of interest

References

1. Jack CR Jr, Knopman DS, Jagust WJ, Shaw LM, Aisen PS, Weiner MW, et al. Hypothetical model of dynamic biomarkers of the Alzheimer's pathological cascade. Lancet Neurol 9 (2010), pp. 119-128.
2. Shim YS, Morris JC. Biomarkers predicting Alzheimer's disease in cognitively normal aging. J Clin Neurol 7 (2011), pp. 60-68.
3. Cummings JL, Morstorf T, Zhong K, Alzheimer's disease drug-development pipeline: few candidates, frequent failures, Alzheimer's Research & Therapy, 6 (2014) 37 doi:10.1186/alzrt269
4. Anderson RM, Hadjichrysanthou C, Evans, S, Wong, MM, Why do so many clinical trials of therapies for Alzheimer's disease fail? Lancet, 390 (2017) pp. 2327-2329 doi:10.1016/S0140-6736(17)32399-1
5. Schott JM, Aisen PS, Cummings JL, Howard RJ, Fox NC. Unsuccessful trials of therapies for Alzheimer's disease. Lancet 2019 393:29 doi:10.1016/S0140-6736(18)31896-8
6. Aisen PS, Petersen RC, Donohue MC, Gamst A, Raman R, Thomas RG, et al. Clinical core of the Alzheimer's Disease neuroimaging initiative: progress and plans. Alzheimer's Dementia *6 (*2010), pp. 239-246.
7. Weiner MW, Aisen PS, Jack CR Jr, Jagust WJ, Trojanowski JQ, Shaw L, et al. The Alzheimer's disease neuroimaging initiative: progress report and future plans. Alzheimer's Dementia*,* 6 (2010) pp. 202-211
8. Qiu Y, Li L, Zhou TY, Lu W, Alzheimer's Disease Neuroimaging Initiative. Alzheimer's disease progression model based on integrated biomarkers and clinical measures. Acta Pharmacol Sin 35 *(*2014), pp. 1111- 1120.
9. Basser PJ, Mattiello J, LeBihan D, MR diffusion tensor spectroscopy and imaging, Biophys. J. 66 (1994) 259–267.
10. Pierpaoli C, Basser PJ, Toward a quantitative assessment of diffusion anisotropy, Magn. Reson. Med. 36 (1996) 893–906.
11. Bozzali M, Cercignani M, Sormani MP, Comi G, Filippi M. Quantification of brain gray matter damage in different ms phenotypes by use of diffusion tensor MR imaging. Am. J. Neuroradiol. 2002;23:985–988
12. ColemanMP, FreemanMR. Wallerian degeneration, wld(s), and nmnat. Annu Rev Neurosci2010;33:245-267.

13. Montal V, Vilaplana E, Alcolea D, Pegueroles J, Pasternak O, González-Ortiz S, et al., Cortical microstructural changes along the Alzheimer's disease continuum, Alzheimers Dement., 14 (2018), pp. 340-351
14. Illán-Gala I, Montal V, Borrego-Écija S, et al. Cortical microstructure in the behavioural variant of frontotemporal dementia: looking beyond atrophy. Brain 2019; 142: 1121– 1133.
15. Lee P, Ryoo H, Park J, Jeong Y, Alzheimer's Disease Neuroimaging Initiative. Morphological and Microstructural Changes of the Hippocampus in Early MCI: A Study Utilizing the Alzheimer's Disease Neuroimaging Initiative Database. J Clin Neurol. 2017 Apr;13(2):144-154.
16. Henf J, Grothe MJ, Brueggen K, Teipel S, Dyrba M. Mean diffusivity in cortical gray matter in Alzheimer's disease: the importance of partial volume correction. Neuroimage Clin. 2018;17:579–86.
17. Lee P, et al., Disruption of gray matter microstructure in Alzheimer's disease continuum using fiber orientation, 2019 International Conference of Korean Dementia Association, 133, FP-0007.
18. McKavanagh R, Torso M, Jenkinson M, et al. Relating diffusion tensor imaging measurements to microstructural quantities in the cerebral cortex in multiple sclerosis. Hum Brain Mapp. 2019; 40: 4417– 4431. https://doi.org/10.1002/hbm.24711
19. Eaton-Rosen Z, Scherrer B, Melbourne A, Ourselin S, Neil JJ, Warfield SK, Investigating the maturation of microstructure and radial orientation in the preterm human cortex with diffusion MRI, Neuroimage, 162 (2017), pp. 65-72
20. Kroenke CD, Using diffusion anisotropy to study cerebral cortical gray matter development, J. Mag. Res. 292 (2018), pp. 106-116
21. Dean DC III, O'Muircheartaigh J, Dirks H, et al. Mapping an index of the myelin g-ratio in infants using magnetic resonance imaging. Neuroimage. 2016; 132: 225- 237
22. McNab, Jennifer A et al. Surface based analysis of diffusion orientation for identifying architectonic domains in the in vivo human cortex. NeuroImage vol. 69 (2013): 87-100. doi:10.1016/j.neuroimage.2012.11.065
23. Cardillo G, ROC curve: compute a Receiver Operating Characteristics curve. Github. https://github.com/dnafinder/roc. 2020
24. Fukutomi H, Glasser MF, Zhang H, Autio JA, Coalson TS, Okada T, et al. Neurite imaging reveals microstructural variations in human cerebral cortical gray matter Neuroimage, 182 (2018), pp. 488-499
25. Wu D et al. Localized diffusion magnetic resonance micro-imaging of the live mouse brain. NeuroImage vol. 91 (2014): 12-20. doi:10.1016/j.neuroimage.2014.01.014
26. Szczepankiewicz F et al. Quantification of microscopic diffusion anisotropy disentangles effects of orientation dispersion from microstructure: applications in healthy volunteers and in brain tumors. NeuroImage vol. 104 (2015): 241-52. doi:10.1016/j.neuroimage.2014.09.057
27. Koo BB, Hua N, Choi CH, Ronen I, Lee JM, Kim DS (2009) A framework to analyze partial volume effect on gray matter mean diffusivity measurements. Neuroimage 44:136–144,

doi:10.1016/j.neuroimage.2008.07.064

28. Truong TK, Guidon A, and Song AW. (2014). Cortical depth dependence of the diffusion anisotropy in the human cortical gray matter in vivo. PLoS ONE 9:e91424. doi: 10.1371/journal.pone.0091424
29. Marín-Padilla M, Ontogenesis of the pyramidal cell of the mammalian neocortex and developmental cytoarchitectonics: a unifying theory. J Comp Neurol. 1992 Jul 8; 321(2):223-40.
30. Callaway EM, Katz LC, Emergence and refinement of clustered horizontal connections in cat striate cortex. J Neurosci. 1990 Apr; 10(4):1134-53.
31. Ghosh A, Shatz CJ. A role for subplate neurons in the patterning of connections from thalamus to neocortex. Development. 1993;117:1031–1047.
32. Rivkin MJ, Flax J, Mozell R, Osathanondh R, Volpe JJ, Villa-Komaroff L, Oligodendroglial development in human fetal cerebrum. Ann Neurol. 1995 Jul; 38(1):92-101.
33. Hardy RJ, Friedrich VL Jr, Oligodendrocyte progenitors are generated throughout the embryonic mouse brain, but differentiate in restricted foci. Development. 1996 122:2059-2069.
34. Pegueroles J, Vilaplana E, Montal V, Sampedro F, Alcolea D, Carmona-iragui M, et al. Longitudinal brain structural changes in preclinical Alzheimer disease Alzheimers Dement, 13 (2017), pp. 499-509
35. Vogt N et al., Cortical Microstructural Alterations in Mild Cognitive Impairment and Alzheimer's Disease Dementia, Cerebral Cortex, Volume 30, Issue 5, May 2020, Pages 2948–2960, https://doi.org/10.1093/cercor/bhz286
36. Marzban EN, Eldeib AM, Yassine IA, Kadah YM, for the Alzheimer's Disease Neurodegenerative Initiative (2020) Alzheimer's disease diagnosis from diffusion tensor images using convolutional neural networks. PLOS ONE 15(3): e0230409. https://doi.org/10.1371/journal.pone.0230409
37. Wen J, Samper-gonzalez J, Bottani S, Routier A, Burgos N, Jacquemont T, et al. Reproducible evaluation of diffusion MRI features for automatic classification of patients with Alzheimer's disease. 2018; Available from: https://arxiv.org/abs/1812.11183
38. Fortin JP, Parker D, Tunc B, Watanabe T, Elliott MA, Ruparel k, Roalf DR, Satterthwaite TD, Gur RC, Gur RE, Schultz RT, Verma R, Shinohara RT, Harmonization of multi-site diffusion tensor imaging data, Neuroimage, 161 (2017), pp. 149-170
39. Jack CR Jr. et al. NIA-AA research framework: toward a biological definition of Alzheimer's disease. Alzheimers Dement. 14, 535–562 (2018).

Table

Table 1. Demographics

	CN (n=78)	EMCI (n=50)	EMCI Non-converter (n=38)	EMCI Converter (n=12)	LMCI (n=34)	AD (n=39)	Post hoc
Female, n (%)	42 (53.8)	19 (37.2)	14 (36.8)	5 (41.7)	15 (44.1)	17 (43.6)	--
Age (SD) (y)	72.7±5.9	74.7±5.3	74.1±4.9	76.4±4.7	73.9±5.6	74.7±7.2	--
Education (SD) (y)	16.7±2.5	15.2±2.6	15.0±2.5	15.6±3.1	16.1±2.8	15.4±2.9	--
GCDR (SD)	0.0	0.5	0.5	0.5	0.5	0.8±0.3	CN<EMCI=LMCI<AD
MMSE (SD)	29.3±1.5	28.2±1.2	28.3±1.1	28.1±1.7	27.6±1.4	24.4±4.0	CN>EMCI=LMCI>AD
MADAS-Cog (SD)	9.7±6.8	13.6±5.9	13.2±5.0	14.5±4.9	14.6±4.8	26.3±14.2	CN<EMCI=LMCI<AD
Immediate recall (SD)	14.2±2.9	10.4±3.4	10.5±3.6	9.9±2.7	6.4±3.3	3.8±2.0	CN>EMCI>LMCI>AD
Delayed recall (SD)	12.8±3.4	8.6±2.0	8.6±2.1	8.7±1.6	3.1±2.7	1.3±1.6	CN>EMCI>LMCI>AD
MRI center	30/48	40/10	29/9	11/1	28/6	36/3	--
Florbetapir+, n (%)	0 (0)	50 (100)	38 (100)	12 (100)	34 (100)	39 (100)	--
AV1451 image, n (%)	44 (68.8)	9 (14.1)	8 (21.1)	1 (8.33)	5 (7.8)	3 (4.7)	--

Data are n (%) or mean±SD values. There were no gender, age, or year of education intergroup differences. GCDR, MMSE, and MADAS-Cog scores in EMCI and LMCI did not show significant differences. Analysis of variance with Tukey test was used for post hoc analysis with p-value < 0.05. For MRI data, two major scanners were used: GE and SIEMENS and delineated as MRI center GE/SIEMENS.

AD: Alzheimer's disease, CN: cognitive normal, EMCI: early mild cognitive impairment, GCDR: global Clinical Dementia Rating, LMCI: late mild cognitive impairment, MADAS-Cog: Modified Alzheimer's Disease Assessment Scale-Cognitive subscale, MMSE: Mini Mental State Examination.

Figures

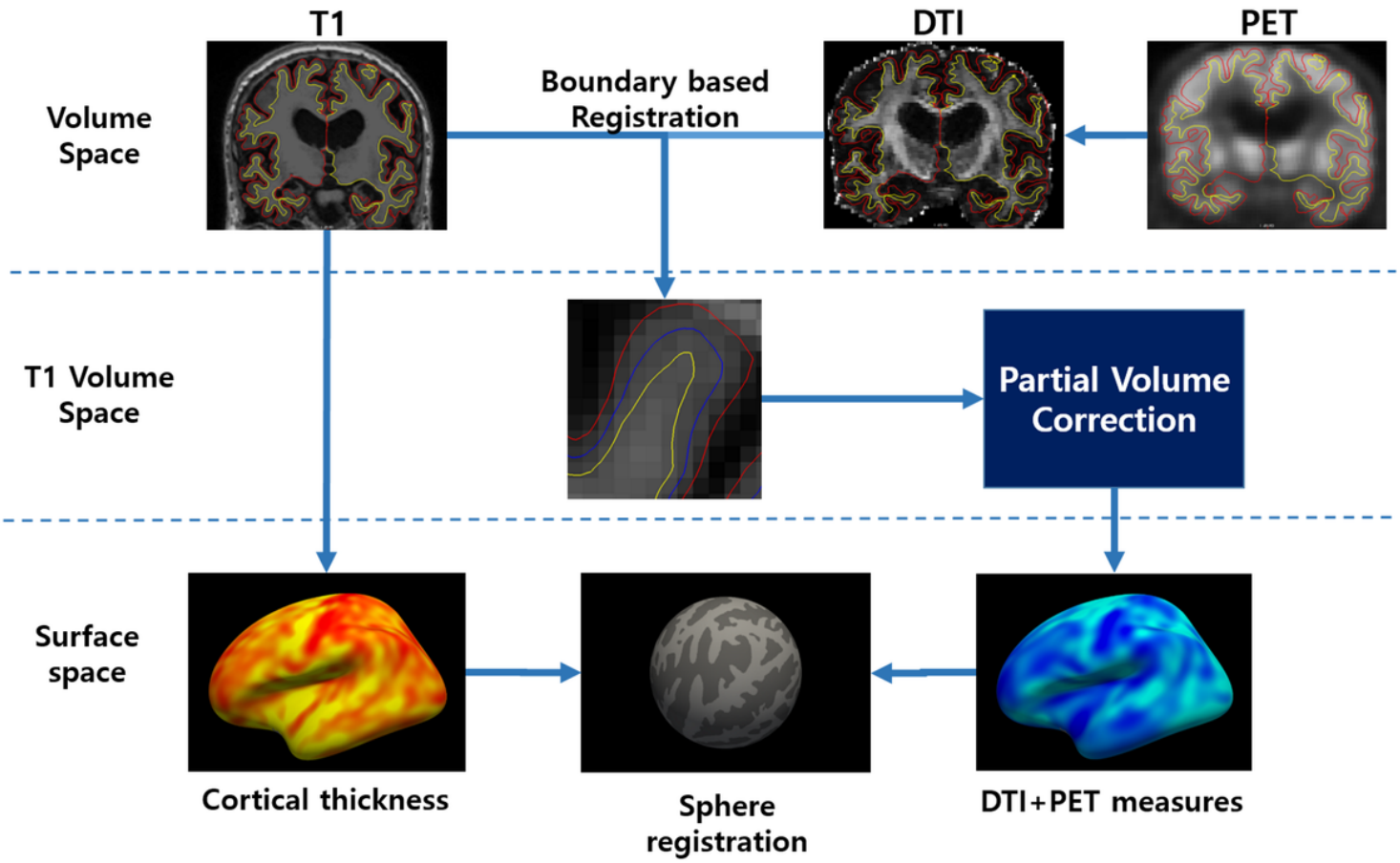

Figure 1

Overall scheme for surface projection analysis. DTI and PET images were boundary-based registered to T1 image and projected to fsaverage surface for group comparison.

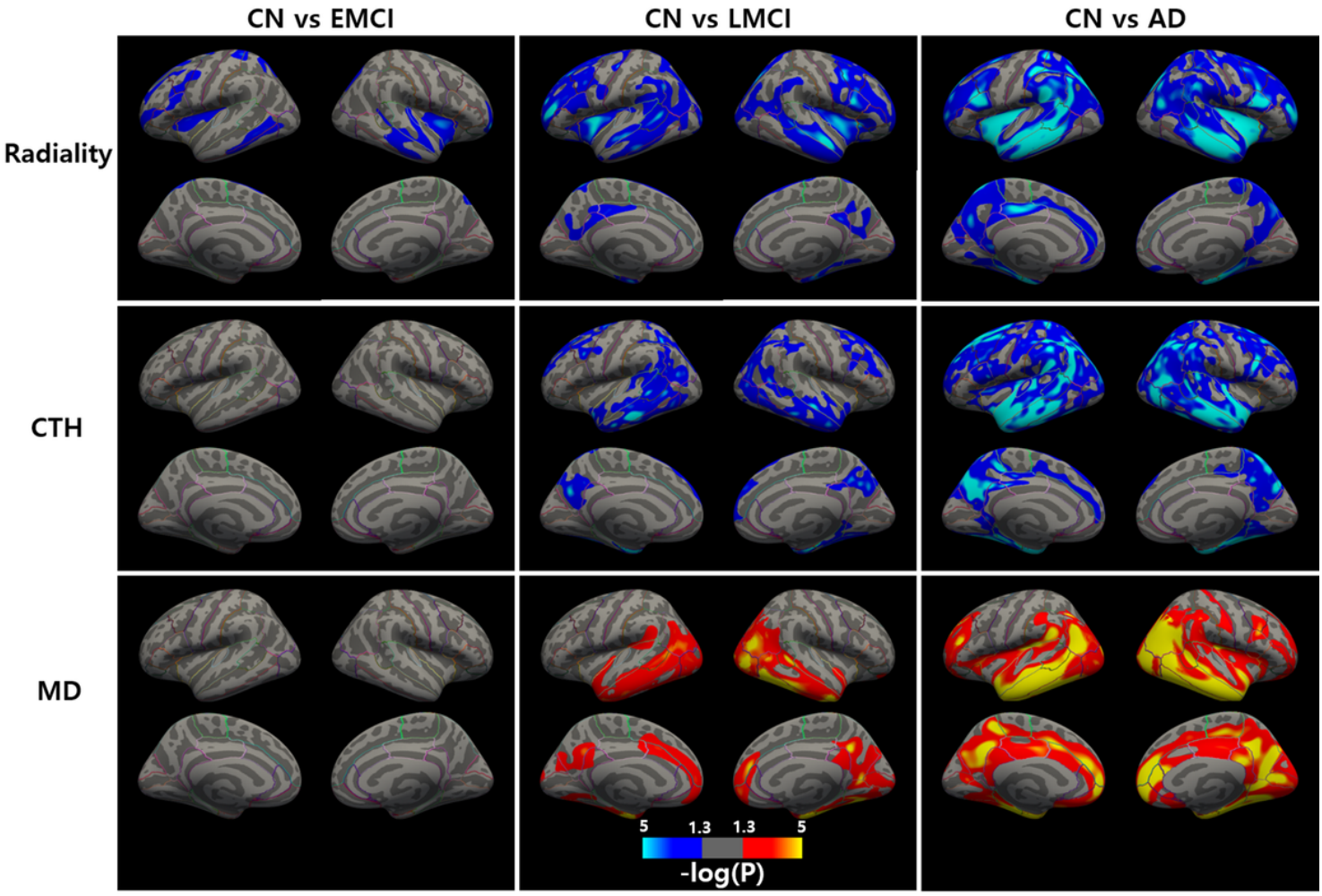

Figure 2

Group differences in radiality, cortical thickness, and mean diffusivity From left to right: CN vs EMCI, CN vs LMCI, and CN vs AD. Blue cluster shows decrease in metrics and red cluster shows increase in metrics. All the cluster were FWE corrected for p-value <0.05. Color bar indicates p-value interval of 0.05 to 10-5

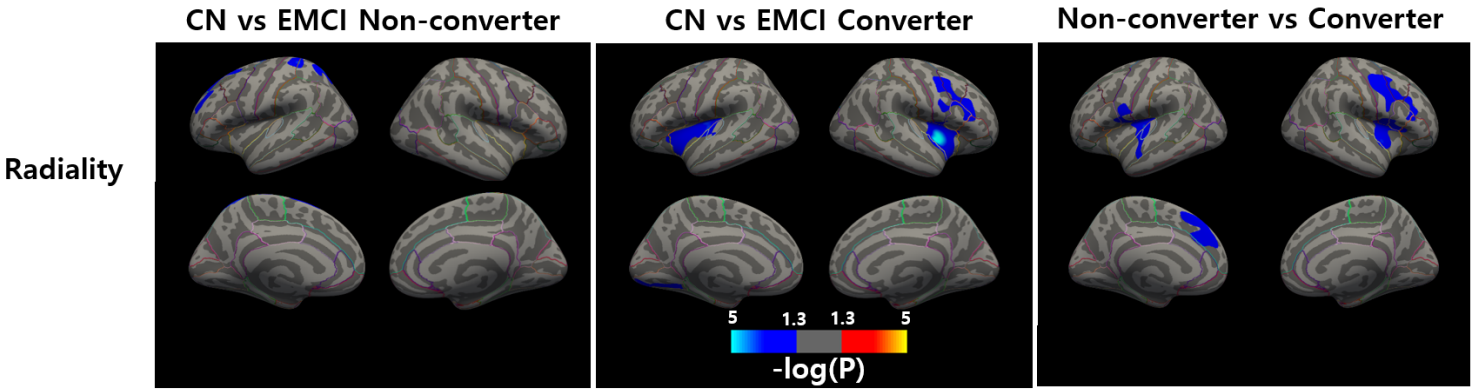

Figure 3

EMCI non-converter and converter differences in radiality From left to right: CN vs EMCI non-converter, CN vs EMCI converter, and non-converter vs converter. Blue cluster shows decrease in metrics and red cluster

shows increase in metrics. All the cluster were FWE corrected for p-value <0.05. Color bar indicates p-value interval of 0.05 to 10-5

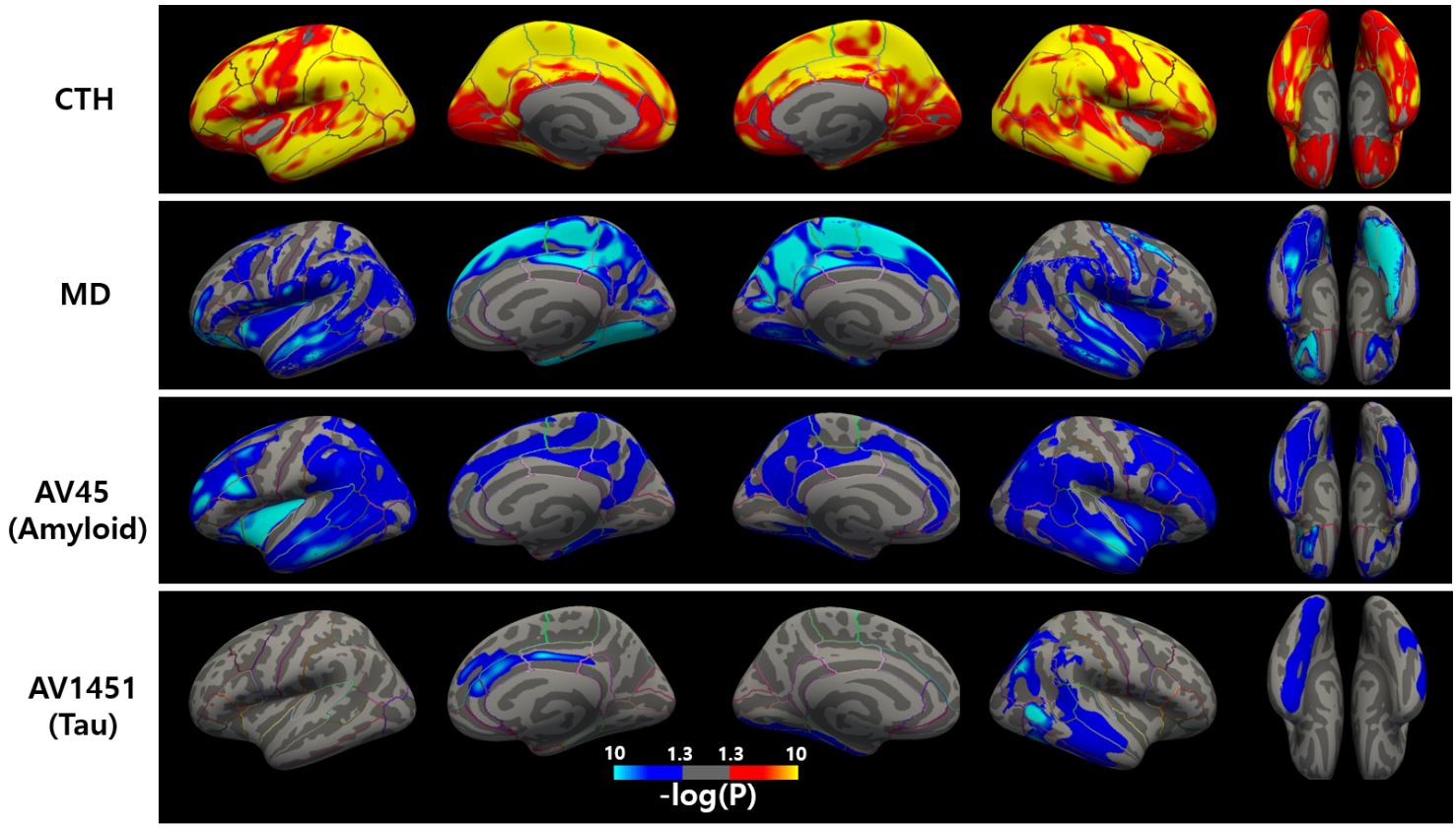

Figure 4

Partial correlation between radiality and image biomarkers. Red cluster shows positive correlation with radiality and blue cluster shows negative correlation. Cortical thickness showed positive correlations, mean diffusivity, AV45, and AV1451 showed negative correlations. Color bar indicates p-value interval of 0.05 to 10-10

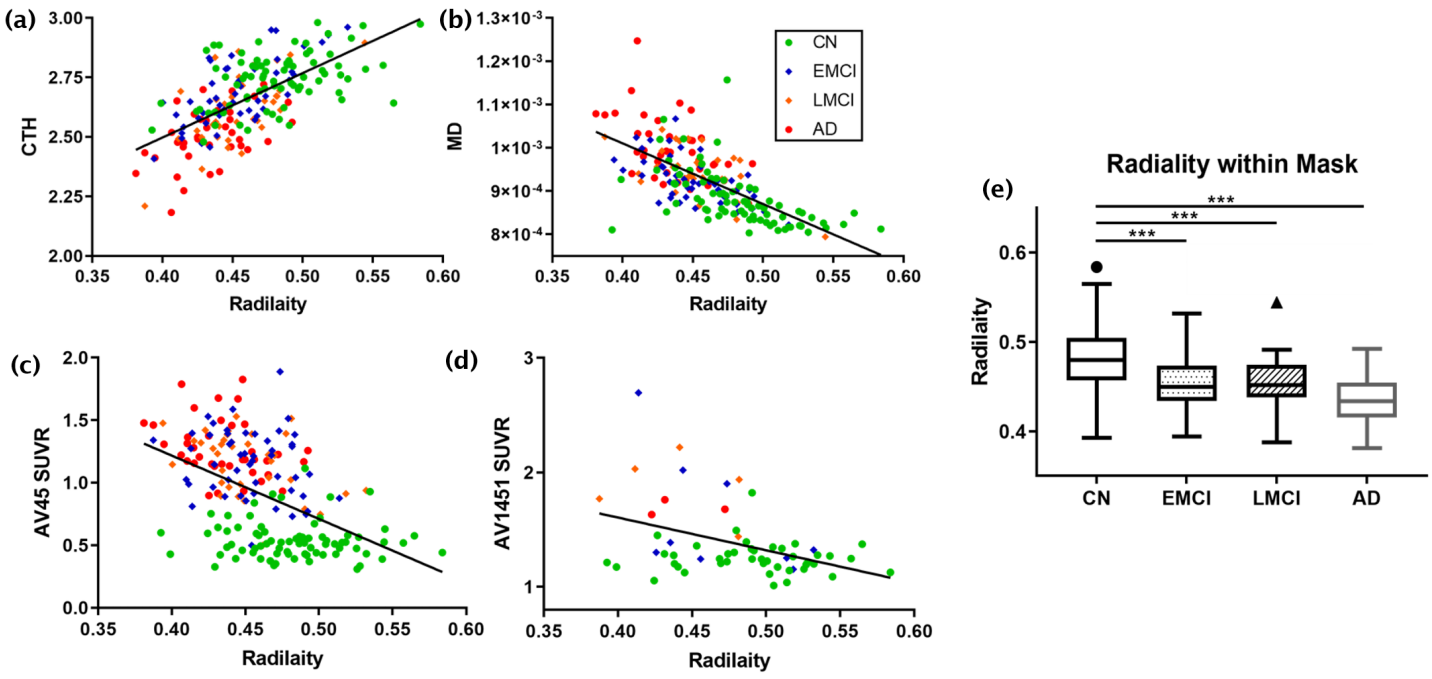

Figure 5

Correlation between radiality with other biomarkers (a) ~ (d) Scatter plot between image biomarkers and radiality. Radiality showed high association with conventional biomarker, indicating that it reflects neuropathology of AD (a) CTh, (b) MD, (c) AV45, (d) AV1451 respectively. (e) Box plot of group radiality comparison within AD specific ROI. Radiality from CN showed significant differences with EMCI, LMCI, and AD with p-value <0.001. There were no differences between EMCI and LMCI.

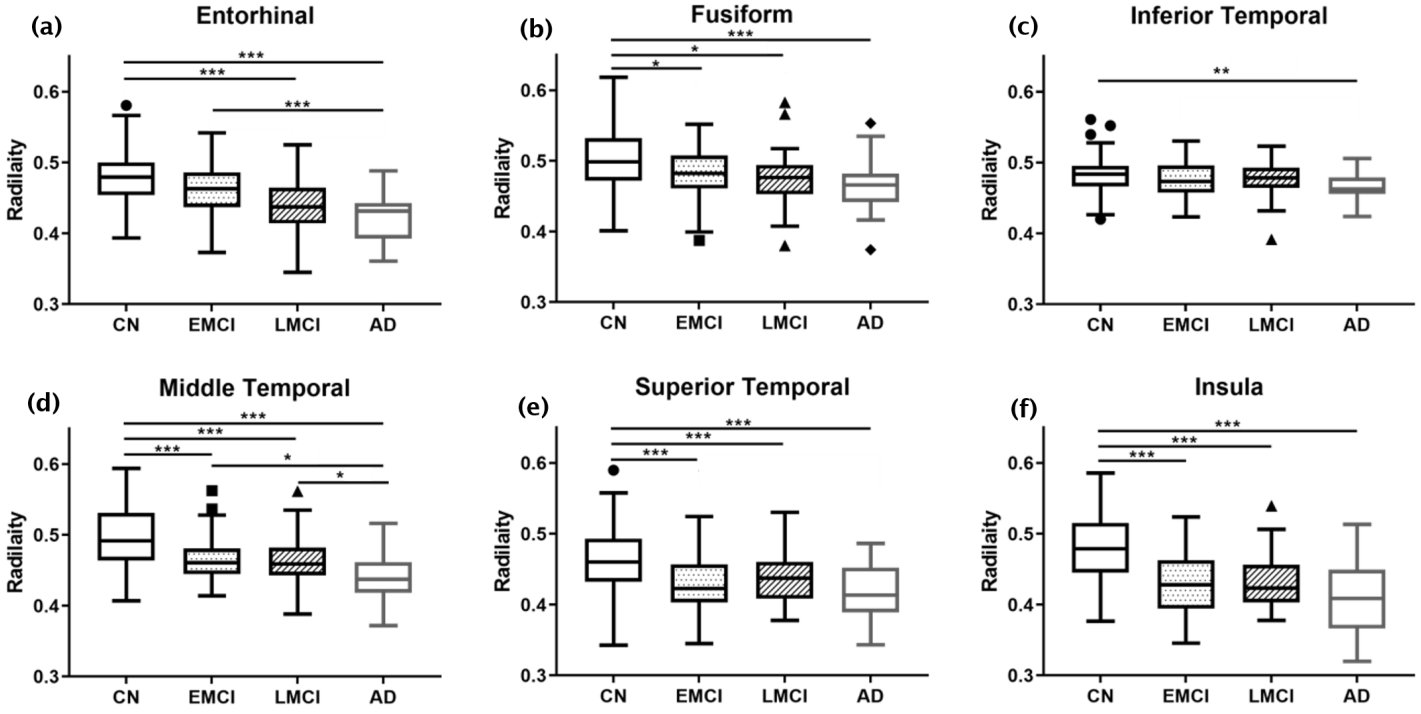

Figure 6

Box plot of group radiality comparison within AD specific ROI. (a) Entorhinal, (b) fusiform, (c) inferior temporal, (d) middle temporal, (e) superior temporal, (f) insula cortex. Significance was tested using one-way ANOVA with * p-value < 0.05, ** p-value < 0.01, *** p-value < 0.001.

Supplementary Files

This is a list of supplementary files associated with this preprint. Click to download.

- Supplementarymaterials.docx
- formula1.docx